DOI 10.1007/s10812-020-01079-y
Journal of Applied Spectroscopy, Vol. 87, No. 5, November, 2020 (Russian Original Vol. 87, No. 5, September–October, 2020)

OPTICAL AND ELECTROPHYSICAL PROPERTIES OF THIN ZINC OXIDE FILMS DOPED WITH SCANDIUM AND OBTAINED BY LASER DEPOSITION

N. A. Bosak,[a*] A. N. Chumakov,[a] A. A. Shevchenok,[b] L. V. Baran,[c] A. G. Karoza,[a] V. V. Malutina-Bronskaya,[d] T. F. Raichenok,[a] and M. G. Sugak[e]

UDC 621.373.826:539.216.2

Nanostructured thin films on a silicon substrate were obtained by high-frequency pulse-periodic laser action (f ~ 10–15 kHz) with wavelength λ = 1.064 μm and power density q = 85 MW/cm^2 on zinc oxide ceramic doped with scandium oxide in a vacuum chamber with pressure p = 2·10^{-2} mm Hg. The morphology of the obtained films was studied by atomic-force microscopy. Features of the transmission spectra in the visible and near and middle infrared regions were shown. The luminescence spectra obtained by excitation at various wavelengths were practically unchanged. The electrophysical properties of the ZnO + 0.9% Sc_2O_3/Si heterostructure were analyzed. It was established that the main conduction mechanism is current limited by space charge in an oxide film with deep traps.

Keywords*: high-frequency laser irradiation, scandium-doped zinc oxide, thin film structure, transmission spectra, luminescence spectra, electrophysical characteristics.*

Introduction. Zinc oxide is a prospective broad-band semiconductor for the creation of lasers and light-emitting diodes in the UV region of the spectrum. At present laser [1] and magnetron [2, 3] sputtering are widely used for the synthesis of ZnO. In [4] small-dimension zinc oxide structures in gas and liquid media with and without doping additives were formed by thermal evaporation and electric discharge synthesis. The elemental and phase composition, morphology, and luminescence characteristics of the synthesized structures were studied. Laser vaporization of zinc and silver in a solution of ammonium nitrate leads to the formation of zinc oxide with dual acceptor doping, and this was confirmed by x-ray structural analysis, photoluminescence, and Raman spectroscopy (RS) [5]. Thin oxide films have been used successfully both in science and in technology [6–9]. Transparent conducting films of zinc oxide combine relatively high values of optical transmission and electric conductivity and are of great interest for the creation of various optoelectronic instruments and devices [10–12]. Zinc oxide can be used in optoelectronic converters as luminescent material in the form of transparent electrodes, the sensitive layers of gas and biological sensors, catalysts, UV detectors, and x-ray and gamma radiation [13, 14].

Research on thin films of ZnO has been encouraged by the creation of sensors. Their use as the sensitive layers in micro- and nanosensors was based on the results from investigations of their structural, electrical, acoustic, and optical characteristics [15]. The physicochemical characteristics of thin films of ZnO can be controlled by including various doping additives in their compositions [15–17].

In the present work the properties of zinc oxide films doped with 0.9 wt.% of scandium oxide were investigated. The choice of doping additive was based on the high sensitivity of compounds of rare-earth elements (including Sc_2O_3) to various external influences and also by the improved piezoelectric characteristics of thin films of ZnO [16]. The morphology of the ZnO + 0.9% Sc_2O_3 thin films, their volt–ampere (VAC) and volt–faraday (VFC) characteristics, and their transmission, luminescence, and Raman spectra were investigated.

*To whom correspondence should be addressed.

[a]B. I. Stepanov Institute of Physics, National Academy of Sciences of Belarus, Minsk, 220072, Belarus; email: n.bosak@ifanbel.bas-net.by; [b]Belarusian National Technical University, Minsk, 220013, Belarus; email: alexshev56@mail.ru; [c]Belarusian State University, Minsk, 220030, Belarus; email: baran@bsu.by; [d]SSPA "Optics, Optoelectronics, and Laser Technology," Minsk, 220072, Belarus; email: malyutina@oelt.basnet.by; [e]NPC National Academy of Sciences of Belarus for Materials Science, Minsk, 220072, Belarus; email: m.sugak@yandex.ru. Translated from Zhurnal Prikladnoi Spektroskopii, Vol. 87, No. 5, pp. 763–769, September–October, 2020. Original article submitted May 26, 2020.

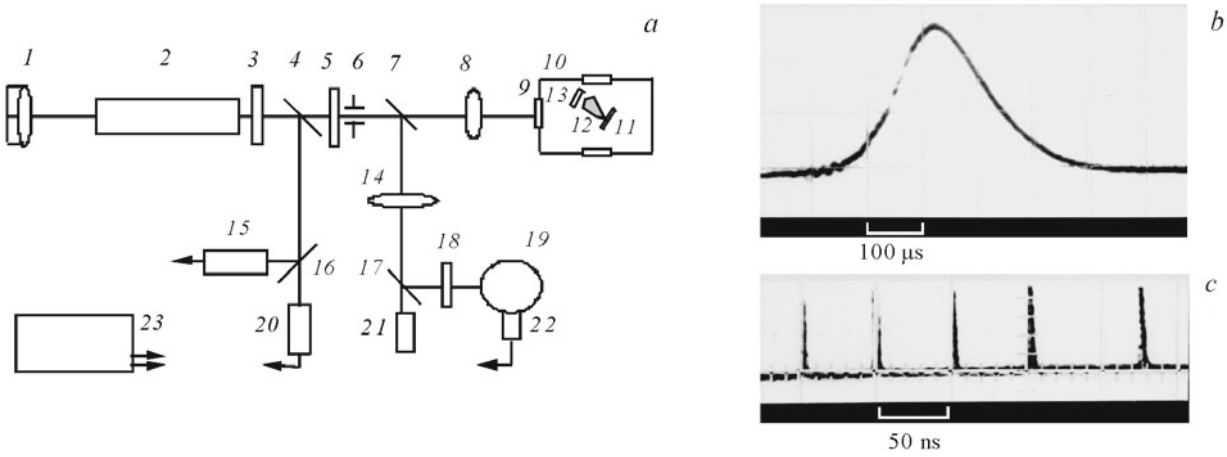

Fig. 1. Diagram of the laser setup (a): 1) passive shutter with LiF: F_2^- color centers, combined with a totally reflecting mirror: 2) active element on neodymium glass; 3) outlet window; 4, 7, 16, 17) beam splitters; 5, 18) optical filters; 6) diaphragm; 8, 14) focusing lenses; 9) inlet window; 10) vacuum chamber; 11) target; 12) plasma torch; 13) silicon substrate; 15), 20) FK-19 photocells; 19) integrating sphere; 21) IMO-2N energy meter; 22) FD-10G photodiode; 23) oscillograph block; b) series of pulses generated by laser with passive shutter; c) form of individual laser pulse.

Experimental Setup and Procedures. An experimental setup (Fig. 1a) based on an industrial GOS-1001 laser (2) was created in order to investigate the characteristics of high-frequency multipulse laser action on metals and composite materials at atmospheric, reduced, and increased pressure. The use of a hemispherical resonator with removable mirrors (a totally reflecting mirror 1 with radius of curvature of 2.5 m and a planar semitransparent mirror 3 with coefficient of reflection $R \approx 37\%$, $\lambda = 1.064$ μm) secured the production of quasicontinuous laser pulses or a series of repeating laser pulses with duration of ~1 μs depending on the alignment of the resonator. However, it was only possible to obtain a regime of regular pulses of laser emission (LE) with duration of ~85 μs (Fig. 1c) at half-height with controllable repetition frequency from 5 to 50 kHz (Fig. 1b) by using a large-scale switch of irradiated lithium fluoride with color centers 1.

To initiate the surface plasma the LE was focused by lens 8 with focal distance $f = 62$ mm onto the surface of the irradiated materials 11 to a relatively uniform spot 2 mm in diameter. The energy was measured and the form of the pulses of the LE was recorded on an IMO-2N energy meter 21 and a photodetector based on FK-19 photocells 15 and 20 and an FD-10G photodiode 22, the signals of which were delivered to C8-14 and C8-13 memory oscillographs. The power density of the LE at the surface of the target was varied in the range of 10^5–10^9 W/cm^2 by means of neutral light filters 8. For experiments over a wide range of air pressures the apparatus included a vacuum chamber 10 with a device for extracting air to $2 \cdot 10^{-2}$ mm Hg. An effective erosion plasma formation method was used to achieve multipulse high-frequency laser action on the surface of the target [18]. Deposition of macroscopically uniform thin films of ZnO with Sc_2O_3 doping additions on the silicon substrate 13 was achieved with LE power density $q = 85$ MW/cm^2 and pulse repetition frequency $f \sim 19$–15 kHz. In order to obtain a multipulse regime of laser generation with high repetition pulse frequency a passive optical shutter of irradiated crystalline lithium fluoride LiF with F_2^- color centers was placed in the resonator close to the removable mirror. The repetition frequency of the laser pulses was changed by varying the pumping level of the laser and the optical density of the shutter.

The starting material for preparation of the targets was analytically pure zinc oxide (supplied by Belreakhim). Analysis of the degree of purity, elemental composition, particle form, and size distribution showed that the initial ZnO powder contained 99.96% of the main substance with a total impurity content of ≤0.04 wt. %. The weight percentage in the powder was 80.3% for zinc and 19.7% for oxygen. The zinc oxide particles in the bulk material had elongated form with length 0.2–0.5 μm, width 0.2–0.4 μm, average size 0.3 μm, and form factor ~0.85. The specific surface area, measured by the Brunauer–Emmett–Teller method, was 3.5 m^2/g for the initial zinc oxide powder and 5.3 m^2/g for the ground material. According to scanning microscopy the Sc_2O_3 powder (of special purity grade) represented plates 5–10-μm-long and

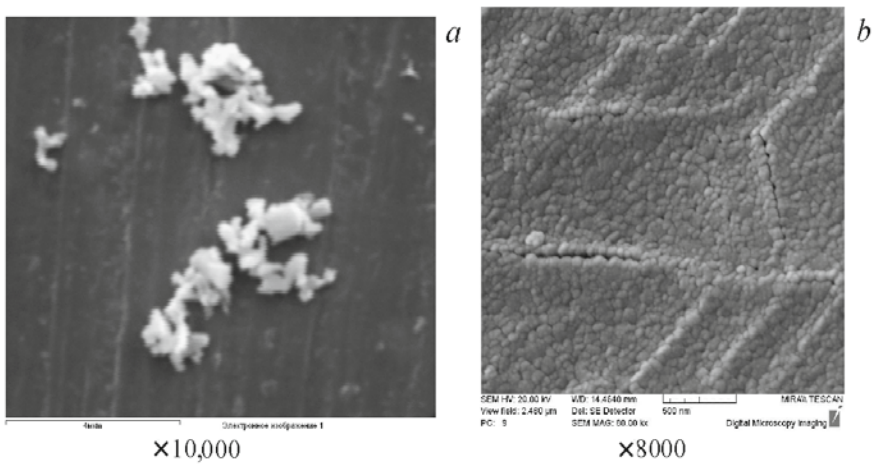

Fig. 2. Form and surface topography of the zinc oxide powder (a) and doping additive Sc_2O_3 (b).

~1-μm-thick and consisted of nanoparticles of ~50 nm. The surface form and topography of the initial zinc oxide powder and the doping additive Sc_2O_3 are shown in Fig. 2 at various magnifications.

The experiments on homogenization and mixing of the powders were carried out in ethyl alcohol in a "SAND" planetary ball mill with chalcedon balls and with cups at a rotation rate of 340 min^{-1} for 2 h. The deposited ceramic targets were obtained by static molding on a ZD-40 press at a pressure of 500 MPa and were baked in a VTP 12/15 laboratory chamber electric furnace in air for 2 h at 1150^{o}C.

The structure of the thin films of doped zinc oxide, produced on glass and silica substrates KDB-12 (100), was studied by atomic-force microscopy (AFM) with a Solver P47 PRO scanning probe microscope. Contactless silicon cantilevers with hardness ratio of 2.5–10 N/m, resonance frequency 115–190 kHz, and needle point rounded radius <10 nm were used. The surface topography was investigated by the force constant method.

The VAC and VFC measurements were made on a laboratory bench based on measurement of emmitance E7-20 at room temperature with and without illumination (a photodiode with λ = 625 nm). These characteristics were recorded with regional shift from −10 to +10 V. The frequency of the signal in the measurement of the VFC was 50 kHz and 1 MHz. The transmission of optical radiation by the thin films in the near IR region was measured on a Carry 500 Scan spectrophotometer. The transmission spectra in the middle IR region were recorded on a NEXUS IR Fourier spectrometer (Thermo Nicolet) in the region of 400–4000 cm^{-1}, and the Raman spectra were recorded on a NanoFlex spectrometer (monochromator inlet slit 100 μm and objective with 100× magnification) in the region of 50–900 cm^{-1}. The time for accumulation of the signal for recording one spectrum was 60 s. An argon laser with λ = 488 nm and power of 2 mW at the sample was used as excitation source for the Raman spectra. The photoluminescence spectra were recorded on an SM 2203 automated spectrofluorimeter (Solar, Belarus).

Results and Discussion. The morphology of thin films of zinc oxide doped with scandium oxide and produced on KDB-12 (100) silicon substrates is shown in Fig. 3. It was established by AFM that films with nanocrystalline structure are formed during deposition on the silicon substrate. The average lateral dimension of the particles is 25–30 nm, and large conglomerates with diameters of 150–300 nm are observed on the surface, but their amount is insignificant. The average height of the surface relief of the films is ≤25 nm, and the average arithmetical roughness is 4 nm (Fig. 3d). The transmission of the laser-deposited film of ZnO with the addition of Sc_2O_3 amounts to ~3.5% in the near IR region of 1–2.6 μm and ~6% in the middle IR region of 2.5–10 μm (Fig. 4). Such films may find use as light-protection coatings for photosensors in the near and middle IR regions.

The luminescence excitation spectra of the sample of ZnO + 0.9% Sc_2O_3 film on silicon were measured. The luminescence excitation spectrum has two bands with maxima at 260 and 360 nm (Fig. 5a). The luminescence spectra were obtained with excitation by radiation with λ = 260, 280, and 340 nm, corresponding to these two excitation bands, are were practically unchanged in form. This can indicate that only one emission center is responsible for the luminescence characteristics of the ZnO + 0.9% Sc_2O_3 film. Further investigation is needed to establish the nature of the center responsible for the emission. However, on account of the fact that the luminescence of Sc_2O_3 is characterized by the presence of longer-

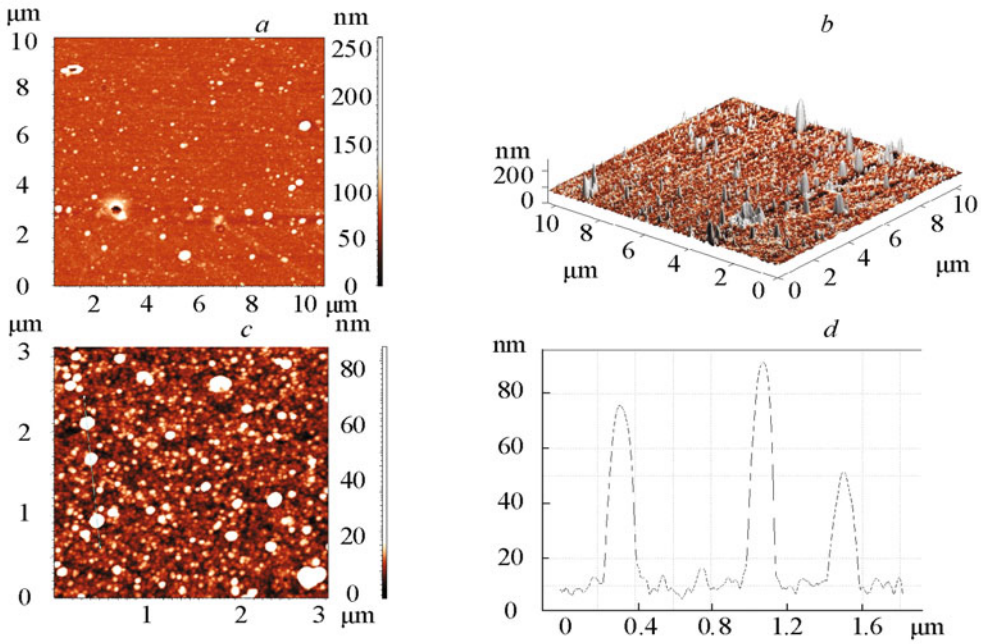

Fig. 3. Surface topography (a–c) and profile of a section along a selected line (d) of laser-deposited thin film of ZnO + 0.9% Sc_2O_3 on a silicon substrate.

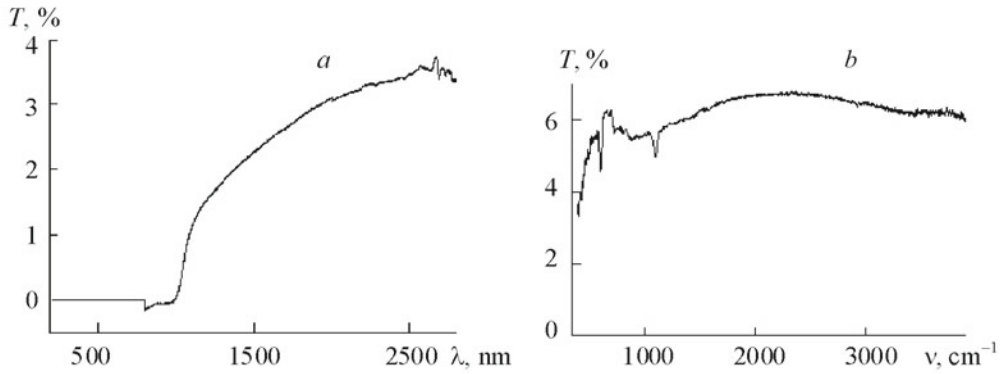

Fig. 4. Transmission spectrum of laser-deposited ZnO + 0.9% Sc_2O_3 film on a silicon substrate in the visible and near (a) and middle (b) IR regions.

wave bands [19] compared with ZnO [20] it can be supposed that scandium oxide Sc_2O_3 may be responsible for the emission from the investigated ZnO + 0.9% Sc_2O_3 film. The Raman spectrum of the zinc oxide thin film doped with scandium oxide on the silicon substrate is presented in Fig. 5b. A strong line for silicon Si 519.7 nm is observed.

The VAC of the ZnO + 0.9% Sc_2O_3 structure on the silicon substrate is presented in Fig. 6a. The dark VAC has a form characteristic of a VAC heterotransition. With a positive shift applied to the electrode it is possible to distinguish three sections on the ZnO + 0.9% Sc_2O_3 film. Each of them is described by an exponential dependence of the current on the potential (characteristic of current with limited space charge in the oxide film and deep traps): $I \sim U^m$. The first ohmic section is observed at voltages of <1.22 V. On the second section 1.22–4 V m = 1.24 and at a voltage of >4 V m = 1.26 (the third section). At a voltage in the order of +1.2 V there is a section with negative differential conductivity that is reproducible in repeated measurements. During illumination with a photodiode at λ = 625 nm in the region of shift from +1 to +6 V the conductivity is rapidly increased by 10 times [21]. The VFC was measured at frequencies of 50 kHz and 1 MHz (Fig. 6b). The high-frequency characteristics at 1 MHz have a form characteristic of a metal–oxide–semiconductor structure on a silicon substrate with *p*-type conductivity. The capacity of the oxide is determined by the high-frequency capacity in the enrichment

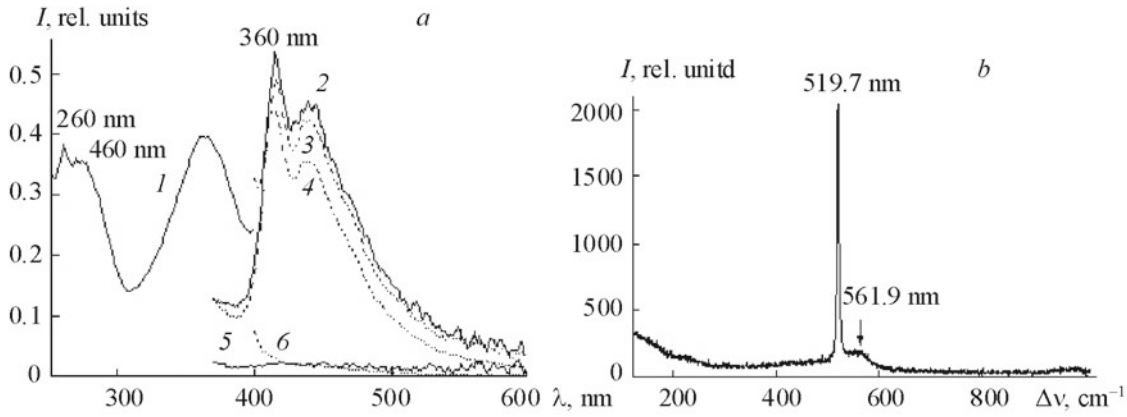

Fig. 5. Luminescence spectra (a) of samples of ZnO + 0.9% Sc_2O_3 film on silicon (2–4) and of silicon substrates (5, 6) at λ_{exc} = 260 (2), 280 (3, 5), and 340 nm (4, 6); 1) luminescence excitation spectrum of sample of film on silicon; λ_{reg} = 460 nm; b) Raman spectrum of thin films on silicon substrate.

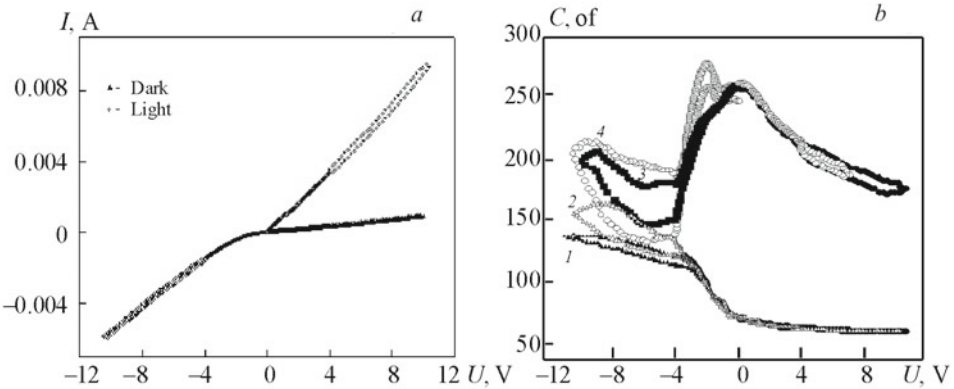

Fig. 6. Volt–ampere (a) and volt–faraday (b) characteristics of the structure with the ZnO + 0.9% Sc_2O_3 film on a silicon substrate; f = 1 MHz, dark (1) and light (2); f = 50 kHz, dark (3) and light (4).

regime (at negative shift voltages from –4 to –11 V). The low-frequency VFC measured at 50 kHz differs from the classical form of VFC for MOS structures. In the region of capacity modulation at low frequency the capacity begins to increase sharply on account of the fact that the energy bands are bent downwards, charge carriers accumulate at the interface, and there can be an effective dynamic exchange of charge between the substrate and the nanostructured film.

Exchange of charge in the course of the measurement period "reduces" the effective thickness of the film, which is reflected in an increase of the differential capacity of the structure. The thickness of the oxide is in the order of about ten nanometers, and tunnel transition through the oxide stimulated by the electronic field is therefore possible, and since there are different permitted states at the boundary of the section, transitions to these levels are possible [22. 23]. At negative potentials a small photoeffect, due to surface states in the oxide, is observed (Fig. 6b).

Conclusions. The results from investigations of the morphology of ZnO + 0.9% Sc_2O_3 thin films, their volt–ampere and volt–faraday characteristics, and the transmission spectra in the visible and near and middle IR regions and the luminescence spectra of samples of the film are presented. Such films may find use as light-protecting coatings for photosensors in the near and middle IR regions. The luminescence spectra, obtained with excitation by radiation with various wavelengths, remain practically unchanged. This shows that only one emission center is responsible for the luminescence characteristics of the ZnO + 0.9% Sc_2O_3 film. A strong silicon line is observed in the Raman spectrum of the thin films. An analysis of the electrophysical characteristics of the ZnO + 0.9% Sc_2O_3 heterostructure is presented. The main conductivity mechanism is

current restricted by space charge in an oxide film with deep traps. During the action of radiation with wavelength of 625 nm the conductivity increases by ten times during change from +1 to +6 V. The dependence of the capacity on voltage at high and low signal frequencies is determined by the thickness of the nanostructured film and the presence of included states.

REFERENCES

1. A. N. Zherikhin, A. I. Khudobenko, R. T. Vill′yams, Dzh. Vilkinson, K. B. User, G. Khiont, and V. V. Voronov, *Kvant. Élektron.,* **33**, No. 11, 975–980 (2003).
2. S.-H. Jeong, B.-S. Kim, and B.-T. Lee, *Appl. Phys. Lett.*, **82**, No. 16, 2625–2627 (2003).
3. T. Minami, T. Yamamoto, and T. Miyata, *Thin Solid Films*, **366**, 63–68 (2000).
4. V. S. Burakov, N. V. Tarasenko, E. A. Nevar, and M. I. Nedel′ko, *Zh. Tekh. Fiz.*, **81**, No. 2, 89–97 (2011).
5. N. Tarasenka, A. Butsen, V. Pankov, T. Velusamy, D. Mariotti, and N. Tarasenko, *Nano-Structures and Nano-Objects*, **12**, 210–219 (2017).
6. X. Yu, T. J. Marks, and A. Facchetti, *Nature Mater. Rev.*, **15**, 383–396 (2016).
7. A. Stadler, *Materials*, No. 5, 661–683 (2012).
8. T. V. Semikina, V. N. Komashchenko, and L. N. Shmyreva, *Élektronika Svyaz*, No. 3, 20–28 (2010).
9. J. F. Wager, D. A. Keszler, and R. E. Presley, *Transparent Electronics*, Springer Science+Business Media, LLC (2008).
10. M. Caglar, S. Ilican, Y. Caglar, and F. Yakuphanoglu, *Appl. Surf. Sci.*, **255**, 4491–4496 (2009)
11. G. V. Lashkarev, V. A. Karpyna, L. I. Ovsiannikova, V. V. Kartuzov, M. V. Dranchuk, M. Godlewski, R. Pietruszka, V. V. Khomyak, and L. I. Petrosyan, *Low Temp. Phys.*, **43**, No. 4, 643–648 (2017).
12. A. A. Bobkov, A. I. Maksimov, P. A. Somov, and E. I. Terukov, *Fiz. Tekh. Poluprovodn.*, **49**, No. 10, 1402–1406 (2015).
13. D. Tainoff, B. Masenelli, O. Boisron, G. Guiraud, and P. Mélinon, *J. Phys. Chem. C*, **112**, 12623–12627 (2008).
14. K. Ellmer, in: D. S. Ginley, H. Hosono, and D. C. Paine (Eds.), *Handbook of Transparent Conductors*, Springer, New York (2010), pp. 193–263.
15. M. É. Bugaeva, V. M. Koval′, V. I. Lazorenko, G. V. Lashkarev, V. A. Karpina, and V. D. Khranovskii, *Sensor. Élektron. Mikrosist. Tekhnol.*, **3**, 34–42 (2005).
16. V. M. Koleshko, A. V. Gulai, A. A. Shevchenok, T. A. Kuznetsova, and M. A. Andreev, *Poroshkov. Metallurg. Respub. Medved. Sb. Nauch. Tr.*, **34**, 106–111 (2011).
17. D.-S. Liu, C.-Y. Wu, C.-S. Sheu, F.-C. Txai, and C. H. Li, *Jpn. J. Appl. Phys.*, **45**(4B), 3531–3536 (2006).
18. L. Ya. Min′ko, A. N. Chumakov, and N. A. Bosak, *Kvant. Élektron.,* **17**, No. 11, 1480–1484 (1990).
19. O. M. Bordun, *J. Appl. Spectrosc.*, **68**, 304–307 (2001).
20. A. M. Ismailov, V. A. Nikitenko, M. R. Rabadanov, L. L. Emiraslanova, I. Sh. Aliev, and M. Kh. Rabadanov, *Vacuum*, **168**, 108854(1–6) (2019).
21. V. V. Malyutina-Bronskaya, V. B. Zaleskii, and T. R. Leonova, *Dokl. BGUIR*, No. 6, 39–43 (2011).
22. M. D. Efremov, G. N. Kamaev, V. A. Volodin, S. A. Arzhannikova, G. A. Kachurin, S. G. Cherkova, A. V. Kretinin, V. V. Malyutina-Bronskaya, and D. V. Marin, *Fiz. Tekh. Poluprovodn.*, **39**, No. 8, 945–951 (2005).
23. V. V. Malyutina-Bronskaya, V. B. Zalesskii, T. R. Leonova, A. I. Belous, and V. I. Plebanovich, *Dokl. BGUIR*, No. 5, 99 (2006).